Arch. Pharm. Chem. Life Sci. 2015, *348*, 113–124

ARCH PHARM
Archiv der Pharmazie

Full Paper

Cytotoxic and Antimicrobial Evaluations of Novel Apoptotic and Anti-Angiogenic Spiro Cyclic 2-Oxindole Derivatives of 2-Amino-tetrahydroquinolin-5-one

Said A. S. Ghozlan[1], Magda F. Mohamed[2], Ahmed G. Ahmed[1], Samia A. Shouman[3], Yasmin M. Attia[3], and Ismail A. Abdelhamid[1]

[1] Department of Chemistry, Faculty of Science, Cairo University, Giza, Egypt
[2] Department of Chemistry (Biochemistry Branch), Faculty of Science, Cairo University, Giza, Egypt
[3] Department of Cancer Biology, National Cancer Institute, Cairo University, Giza, Egypt

A novel series of cyclic 2-oxindole derivatives incorporating 2-amino-tetrahydroquinolin-5-one were prepared. The structures of the prepared compounds were elucidated using different spectral tools. The regio-orientation of the reaction products was elucidated through NOE difference experiments and through using substituents on the *ortho* position to affect further cyclization. Antitumor and antimicrobial evaluations were performed on the prepared compounds. Most of these compounds exhibited high to moderate antimicrobial activity. With respect to the antitumor activity, the compounds showed more potent cytotoxic effect only toward the human breast cancer cell line MCF-7. Also, we found that derivatives containing an ester group (**8c**, **11b**, **14b**, and **15b**) are more active than those containing a cyanide group (**8a**, **11a**, **14a**, and **15a**). Moreover, compounds **15b** and **8b** are the most active derivatives in this group. These two compounds showed apoptotic inhibition of the proliferation of human breast adenocarcinoma MCF-7 cells through DNA fragmentation, induction of the tumor suppressor protein p53, induction of caspase-9, and finally the inhibition of angiogenesis by decreasing vascular endothelial growth factor expression and secretion.

Keywords: 2-Amino-tetrahydroquinolin-5-one / Anti-angiogenesis / Antimicrobial activity / Apoptosis / Cytotoxicity

Received: August 12, 2014; Revised: October 7, 2014; Accepted: November 7, 2014

DOI 10.1002/ardp.201400304

Introduction

The spirooxindole core is one of the most distinguished heterocyclic ring systems, which constitutes the core structural element of many natural and biologically active molecules [1–7]. On the other hand, the 2-amino-tetrahydroquinolin-5-one skeleton also exists in a variety of biologically significant compounds possessing antimicrobial, [8, 9] and anticancer activities [9–13]. Considering the versatile bioactivities of the two structures of spirooxindole and 2-amino-tetrahydroquinolin-5-one, we assume that the integration of the two scaffolds into a spiro-oxindole incorporating 2-amino-tetrahydroquinolin-5-one can result in the discovery of new active drugs. Cancer is uncontrolled proliferation of tumor cells and common cause of death in the world [14]. In particular, human breast cancer is the main reason of women death in developed countries. So, developing new derivatives for tumor treatment is more urgent for both improvement of health care and for the progress of new therapeutic agents, which is more safe and cheap. In this study, different novel spiro-oxindole incorporating 2-amino-tetrahydroquinolin-5-one derivatives were synthesized and tested for antimicrobial and anticancer activity, using a panel of cancer cell lines. In addition, we are interested to explore the molecular mechanism of action that the active spiro-oxindole derivatives follow to inhibit the growth of breast cancer cell line (MCF-7). Two of the active synthesized compounds **15b** and **8b** showed apoptotic inhibition of the proliferation of MCF-7 cells through deoxyribonucleic acid (DNA) fragmentation, induction of caspases, and finally through the inhibition of

Correspondence: Dr. Ismail A. Abdelhamid, Department of Chemistry, Faculty of Science, Cairo University, 12613 Giza, Egypt.
E-mail: ismail_shafy@yahoo.com, ismail.abdelhamid@oci.uni-hannover.de

ARCH PHARM
Archiv der Pharmazie

angiogenesis by decreasing vascular endothelial growth factor (VEGF) expression and secretion. In previous studies, similar compounds cause apoptotic DNA fragmentation and inhibition of the growth of human A549 lung adenocarcinoma [15]. Also they induce the expression of the tumor suppressor p53 protein, which plays an important role in apoptosis, DNA repair, and angiogenesis [16–18]. Caspase-9 is a member of cysteine proteases family (caspases) that have been implicated in apoptosis and cytokine processing. When cells receive apoptotic stimuli, mitochondria release cytochrome *c,* which then binds to Apaf-1. The resultant complex recruits caspase-9, leading to its activation. Activated caspase-9 cleaves downstream caspases, such as caspase-3, -6, and -7, initiating the caspase cascade [19]. The two novel compounds **15b** and **8b** were found to induce apoptosis through the expression of m-RNA of caspase-9 in MCF-7 cells. Finally, in the light of these facts, we hoped from the synthesis of these novel compounds to make link between chemists, biologists, and doctors of medicine, hoping to obtain a promising significant alternatives for anticancer derivatives in the future.

Results and discussion

Synthetic chemistry

In conjunction to our interest in Michael addition reactions to the active double bonds in the α,β-unsaturated nitriles [20–24], the possibility of [3 + 3] atom combination of enamines **3a–d** with 3-cyanomethylidene-2-oxindoles **4a,b** was studied. Thus, the enamines **3a–d** were prepared as reported in literature (Scheme 1) [25] and reacted directly with 3-cyanomethylidene-2-oxindole derivatives **4a,b**. The reaction of the cyclic enamine **3a** with 3-cyanomethylidene-2-oxindoles **4a,b** yields spiroquinolines that may be formulated as **6** or **8**. Compounds **6** result from initial addition of NH to the activated double bond in **4** (pathway A), while compounds **8** result from initial addition of enamine CH to activated double bond in **2** (pathway B). The Nuclear Overhauser Effect (NOE) difference experiment revealed enhancement of aryl protons on irradiating the NH_2 group at $\delta = 5.37$ ppm, and this is in agreement with structure **8** (Scheme 2)

The structure of compounds **8** (pathway B) was also simply elucidated chemically through the direct reaction of the enamine **3b** (carrying methyl ester on the *ortho* position of the benzene ring) with 3-cyanomethylidene 2-oxindoles **4**, where only further cyclization occurred in the case of 2-aminoquinolines **10**, while in the case of 4-aminoquinolines **9** no further cyclization occurred.

Treatment of the cyclic enamine **3b** with **4a** leads to the formation of product of cyclization with methanol elimination to give compound **11** (Scheme 3). The structure of **11** was confirmed based on spectral data. The analyses clearly indicate the absence of the OMe group. The mass spectra of **11a** revealed the molecular-ion peak at *m/z* 436. The ^{1}H-nuclear magnetic resonance (NMR) spectrum of **11a** featured two singlet signals at δ 1.02 ppm and 1.06 ppm for methyl protons. It also showed characteristic multiplets at δ 2.07 ppm assigned to methylene protons. The aromatic protons appeared as multiplets in the region δ 6.78–8.0 ppm. In addition, it indicated a characteristic broad band at δ 11.64 for the NH group. Furthermore, full assignment of the ^{13}C-NMR data confirmed the structure of **11a**, where the key signal at δ (C) 42.4 was assigned to the sp^3. The signals at 151.5, 177.8, and 194.5 were assigned to three carbonyl groups.

In a similar manner, when the cyclic enamine **3c** was treated with 3-cyanomethylidene 2-oxindoles **4a,b** in the presence of 1,8-diazabicyclo[5.4.0]undec-7-ene (DBU) as catalyst over 5 h, the spiro-hexacyclic structure **14a,b** was obtained as the main product, which was characterized spectroscopically (Scheme 4).

Encouraged by the results acquired from enamines **1a–c**, we attempted to expand the scope of this reaction to prepare spiro-heptacyclic structures. Thus, enamine incorporating a tetrahydrothiophene moiety **3d** was prepared.

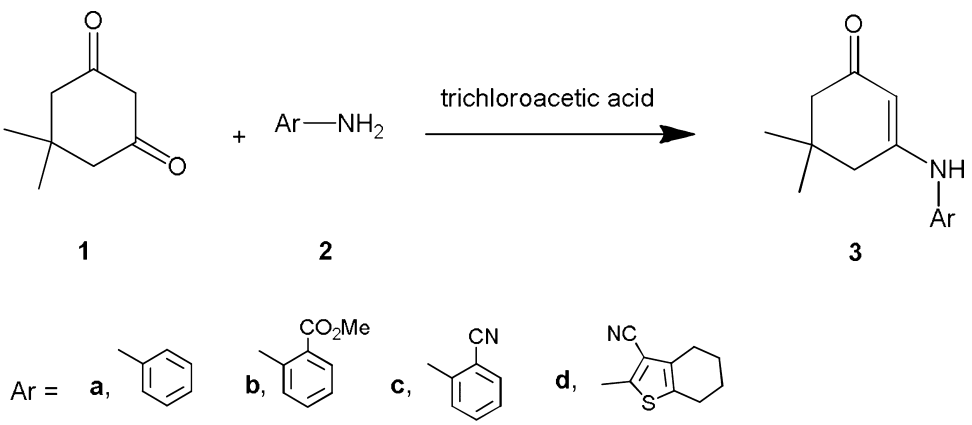

Scheme 1. Synthesis of enamines **3a–d**.

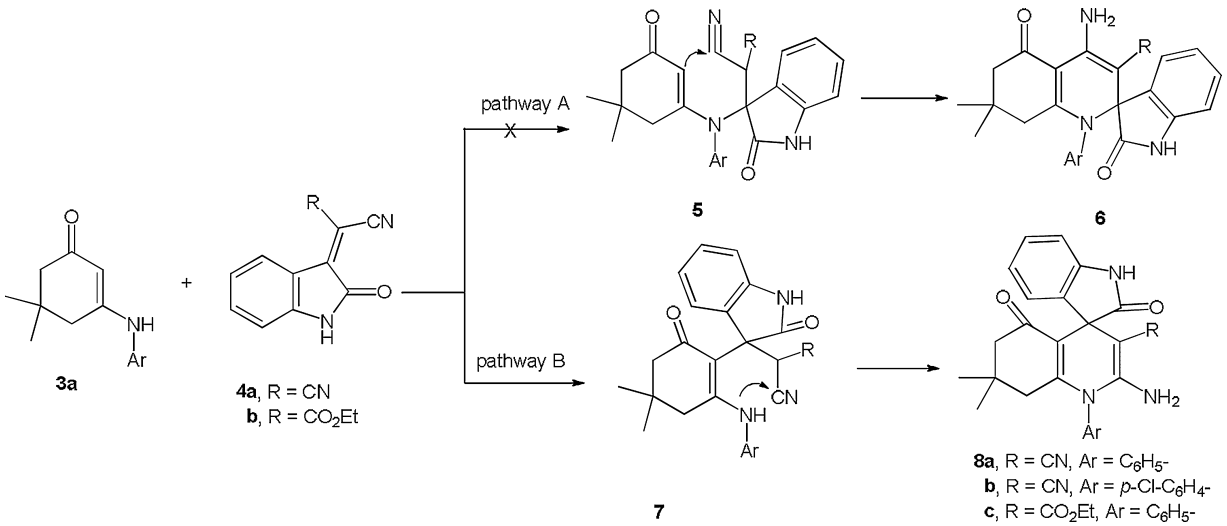

Scheme 2. One-pot synthesis of 1′-(aryl)-7′,7′-dimethyl-2,5′-dioxo-5′,6′,7′,8′-tetrahydro-1′*H*-spiro[indoline-3,4′-quinoline]-3′-carbonitrile (carboxylate) **8a–c**.

The interaction of enamine **3d** with **4a,b** led directly to the formation of the spiro-heptacyclic product **15a,b** (Scheme 5). Compounds **15a,b** were characterized by inspection of their spectroscopic data. The ^{1}H NMR spectrum of **15a** indicated two singlet signals at δ 0.89 and 0.96 for the two methyl groups. It also featured characteristic set of multiplets at δ = 1.84, 2.22, and 2.78 for the methylene protons. It indicated a broad singlet at δ = 6.08 ppm for NH_2. It also revealed aromatic protons as multiplets at δ = 6.77 and 7.13 ppm. In addition, it showed broad singlet at 10.31 ppm for NH. Furthermore, full assignment of the ^{13}C-NMR data confirmed the structure of **13a**, where the key signal at δ = 48.7 was assigned to the spiro-carbon. The signals at 179.7 and 194.6 ppm are assigned to two CO

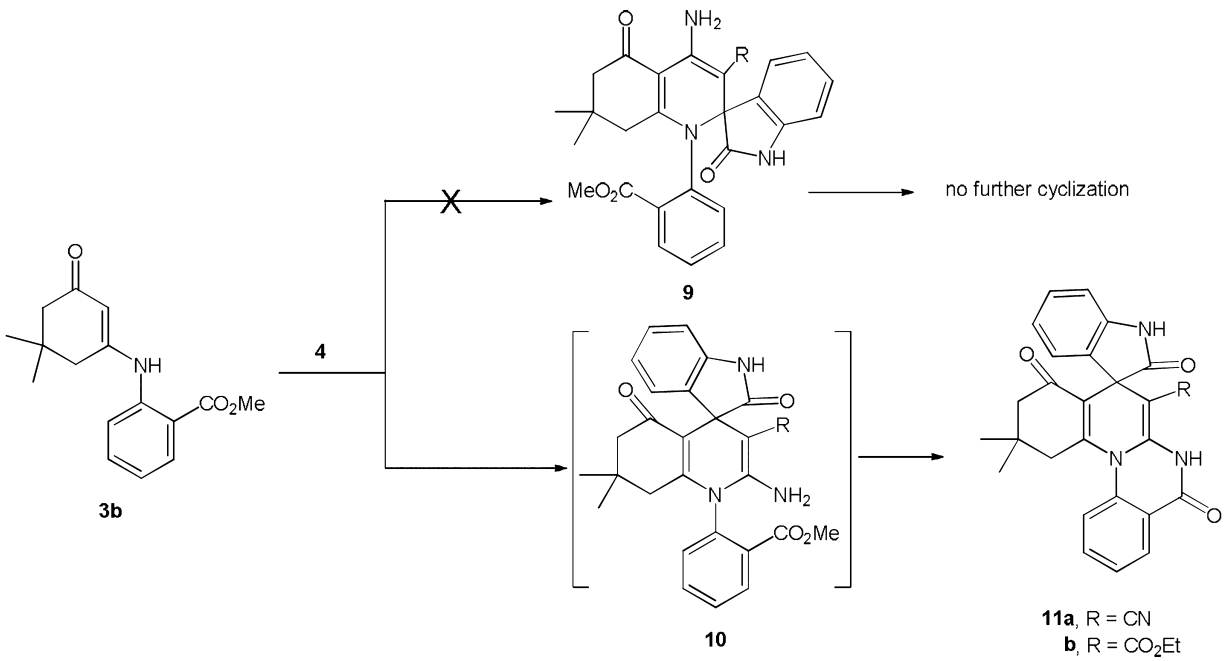

Scheme 3. One-pot synthesis of hexahydrospiro[indoline-3,8′-quinolino[1,2-a]quinazoline]-7′-carbonitrile (carboxylate) **11a,b**.

ARCH PHARM
Archiv der Pharmazie

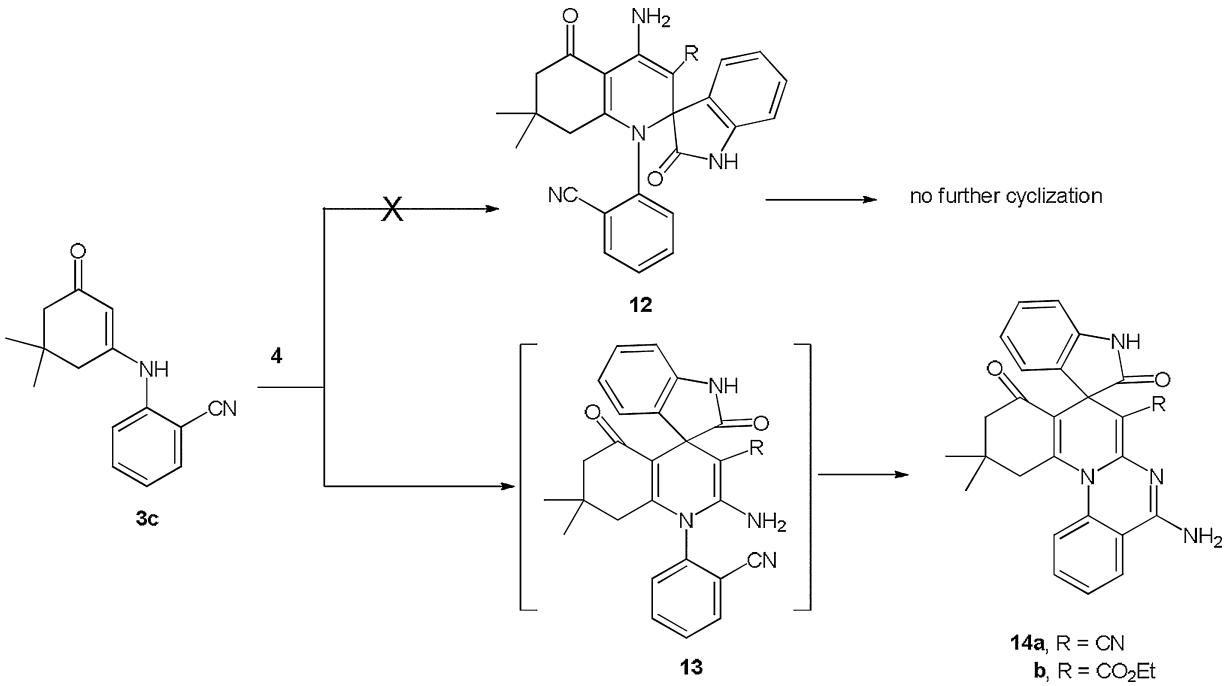

Scheme 4. One-pot synthesis of 5′-amino-tetrahydrospiro[indoline-3,8′-quinolino[1,2-a]quinazoline]-7′-carbonitrile (carboxylate) **14a,b**.

groups. All other carbon signals appeared at their expected positions.

Biology

Antimicrobial activity

The data showed that the derivatives (**11a**, **11b**, **14a**, **14b**, **15a**, **15b**, and **8b**) have different capacity of inhibiting the metabolic growth of the tested bacteria, such as *Bacillus subtilis* and *Staphylococcus aureus* as gram-positive strains and *Escherichia coli* and *Pseudomonas aeuroginosa* as gram-negative bacteria, to different extents using tetracycline as positive antibacterial agent (Table 1). The inhibitory activity of these compounds may be related to their effect on the cell wall structure of the bacteria. This is possible because the cell wall is essential to the survival of bacteria and some antibiotics are able to kill bacteria by inhibiting a step in the synthesis of peptidoglycan [26]. On the other hand, the two compounds **8a** and **8c** exhibited no antibacterial activity toward the tested bacteria. On the other hand, compound **8b** exhibited moderate antibacterial activity due to the presence of Cl in the *para* position of the benzene ring. In addition, compounds **11b** and **14a** show only moderate activity toward the gram-negative bacteria *E. coli.* The size of the inhibition zone (Fig.1) depends upon the incubation conditions, culture medium, rate of diffusion, and the concentration of the antibacterial agent. The compounds

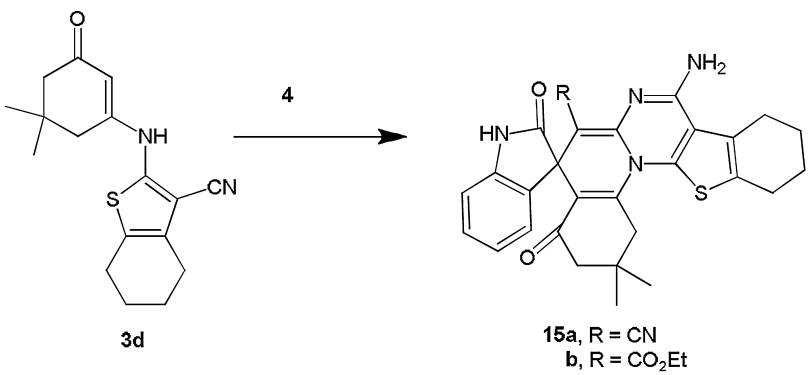

Scheme 5. One-pot synthesis of 8-amino-octahydrospiro[benzo[4′,5′]thieno-[3′,2′:5,6]pyrimido-[1,2-a]quinoline-5,3′-indoline]-6′-carbonitrile (carboxylate) **15a,b**.

Table 1. Antimicrobial activity of a novel series of spiro cyclic 2-oxindole derivatives of 2-amino-tetrahydroquinolin-5-one.

Compounds	Inhibition Diameter Zone (mm)			
	Bacillus subtilis (G^+)	*Staphylococcus aureus* (G^+)	*Escherichia coli* (G^-)	*Pseudomonas aeuroginosa* (G^-)
Negative control (DMSO)	0.0	0.0	0.0	0.0
Positive control (tetracycline)	30	30	33	31
8a	0.0	0.0	0.0	
8b	17	18	15	18
8c	0.0	0.0	0.0	0.0
11a	17	19	18	18
11b	0.0	0.0	18	0.0
14a	0.0	0.0	17	0.0
14b	17	16	17	15
15a	19	20	20	19
15b	22	20	21	19

15b and **15a** exhibited the most potent effect in this series against all types of selected bacterial strains. The remarkable activity of the two compounds against both types of the bacteria, especially when compared to compounds **8a**, **8b**, **8c**, **11a**, **11b**, **14a**, and **14b** may be attributed to the presence of tetrahydrobenzo[*b*]thiophene group, which may bind to some proteins inside cells, especially that contain S atom. In addition, the presence of additional tertiary nitrogen in **15b** and **15a** make these two compounds able to form covalent hydrogen bonding with the active centers of the cell constituents, resulting in interference with the normal cell process. A possible explanation for the poor activity of **8a** and **8c** compounds with respect to other compounds may be attributed to the presence of carbocyclic phenyl group in their structures instead of heterocyclic ring, which represented in other structures. Generally, the replacement of carbocyclic rings with heterocyclic ones decreases the biological activity of the compounds [27]. This may be due to the inability of carbocyclic compounds to form hydrogen bonding as heterocyclic ones with the active centers of cell structures. Furthermore, the less activity may be also related to their low lipophilicity, and this decreases their penetration through the lipid membrane and, consequently, they cannot inhibit the growth of the microorganism. Following **15b** and **15a** in activity are compounds **11a** and **14b**, while **11a** is still more active than **14b**. This may be due to the presence of carboxamide group, which can be converted into enol form. Hence, there will be hydrogen bond with the nucleophilic hydrogen in addition to the presence of tertiary nitrogen.

Anticancer evaluation

The newly synthesized compounds were screened for anticancer activity on two human cancer lines: breast cancer cell line (MCF-7) and hepatocellular carcinoma (HEPG-2). Firstly, all compounds were filtered using concentration 100 μg/mL to predict the most promising compounds that induce more than 70% of survival inhibition. All the tested compounds were evaluated for their toxicity in normal cell line (HBF4) using doxorubicin as positive control (Fig. 2). Our results showed that the tested compounds were more cytotoxic toward human breast cancer MCF-7 than liver cancer HEPG-2 cells (Table 2). The most active derivatives in this series at 100 μg/mL are **8a**, **8c**, **14b**, **15b**, and **8b**. In general, derivatives containing ester group as **8c**, **11b**, **14b**, and **15b** are more active than those containing cyanide group as **8a**, **11a**, **14a**, and **15a**. The compounds **15b** and **8b** are the most active derivatives in this group, which showed very high activity, 80% and 79%, respectively, at 100 μg/mL concentration. The compound **15b** is still the most potent compound than **8b** due to the presence of additional tetrahydrobenzo[*b*]thiophene group. On the other hand, **8b** is more active (79%) than **8a** (76%), where the presence of electron withdrawing group (Cl) in the *para* position of phenyl ring increases the biological activity of **8b**. Also, the compound **11a** is more potent (73%) than **14a** (71%) due the presence of the biologically active carboxamide group. Interestingly, most of our series showed less toxic effect against the normal melanocytes (HBF4) cells as shown in Table 2. In this study, we restricted the investigation of the mechanistic pathways to the most active compounds **15b** and **8b** (Fig. 2) using the concentration of IC_{50} to study their apoptostotic and anti-angiogenic potency.

*Effects of compounds **15b** and **8b** on expression and protein level of VEGF in culture media*

VEGF is one of the important angiogenic factors secreted by the tumor cells, and stimulates the formation of new blood vessels [28]. VEGF-A secretion as indicator for angiogenesis was determined in MCF-7 media by ELISA kit. Figure 3 shows that compounds **15b** and **8b** decrease the VEGF-A secretion in MCF-7 medium following 48 h of exposure. Moreover, these results are confirmed at expression level using reverse-transcriptase polymerase chain reaction (RT-PCR). The results

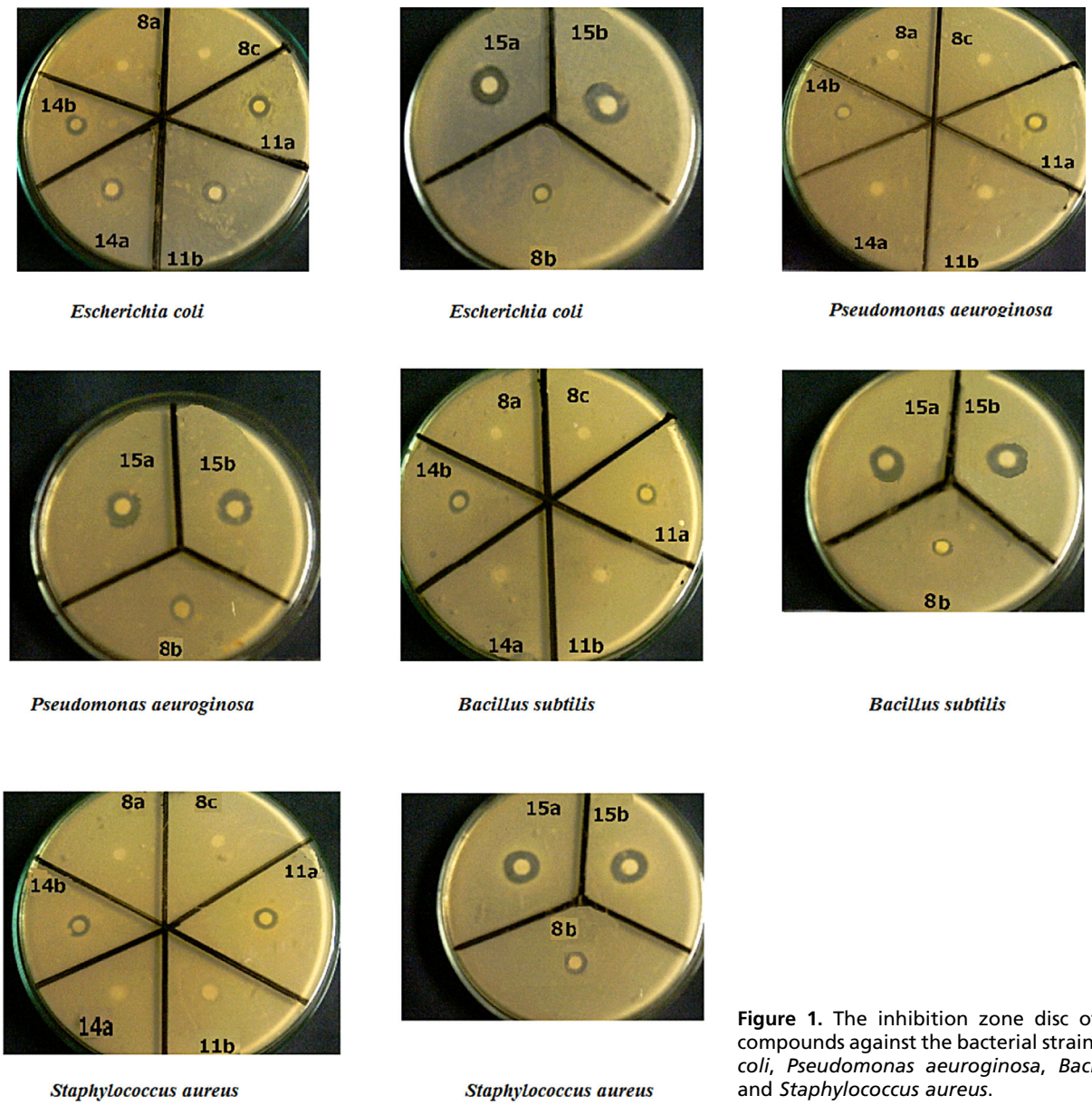

Figure 1. The inhibition zone disc of the tested compounds against the bacterial strains *Escherichia coli*, *Pseudomonas aeuroginosa*, *Bacillus subtilis*, and *Staphylococcus aureus*.

of PCR products showed that a single specific PCR product was obtained with a molecular size of approximately 131 bp for VEGF-coding gene. There was downregulation in the m-RNA of VEGF by both compounds **15b** and **8b** in MCF-7 cells (Fig. 4). β-Actin gene, which separated at approximately 550 bp, was used as housekeeping gene in this experiment.

Expression of caspase-9 and tumor suppressor p53 by RT-PCR analysis

A RT-PCR was done to measure the relative levels of mRNA expression for both p53 and caspase-9 as indicator for apoptosis. Figure 4 shows that the two derivatives at their IC_{50} values **15b** (14.2 μM/mL) and **8b** (23 μM/mL) induce the expression of the tumor suppressor p53 protein, which plays an important role in apoptosis, but the m-RNA expression level of MCF-7 cells treated with compound **15b** is much more than that of compound **8b**. Apoptosis is a genetically programed mechanism that allows the cell to commit suicide [29]. Caspases are essential in apoptosis (programmed cell death) of cells for the development and survival of the organism. Also, our results revealed that the two compounds **15b** and **8b** induce apoptosis through the expression of m-RNA of caspase-9 in the tumor cells as shown in Fig. 4, where there is no expression appearing in the control sample.

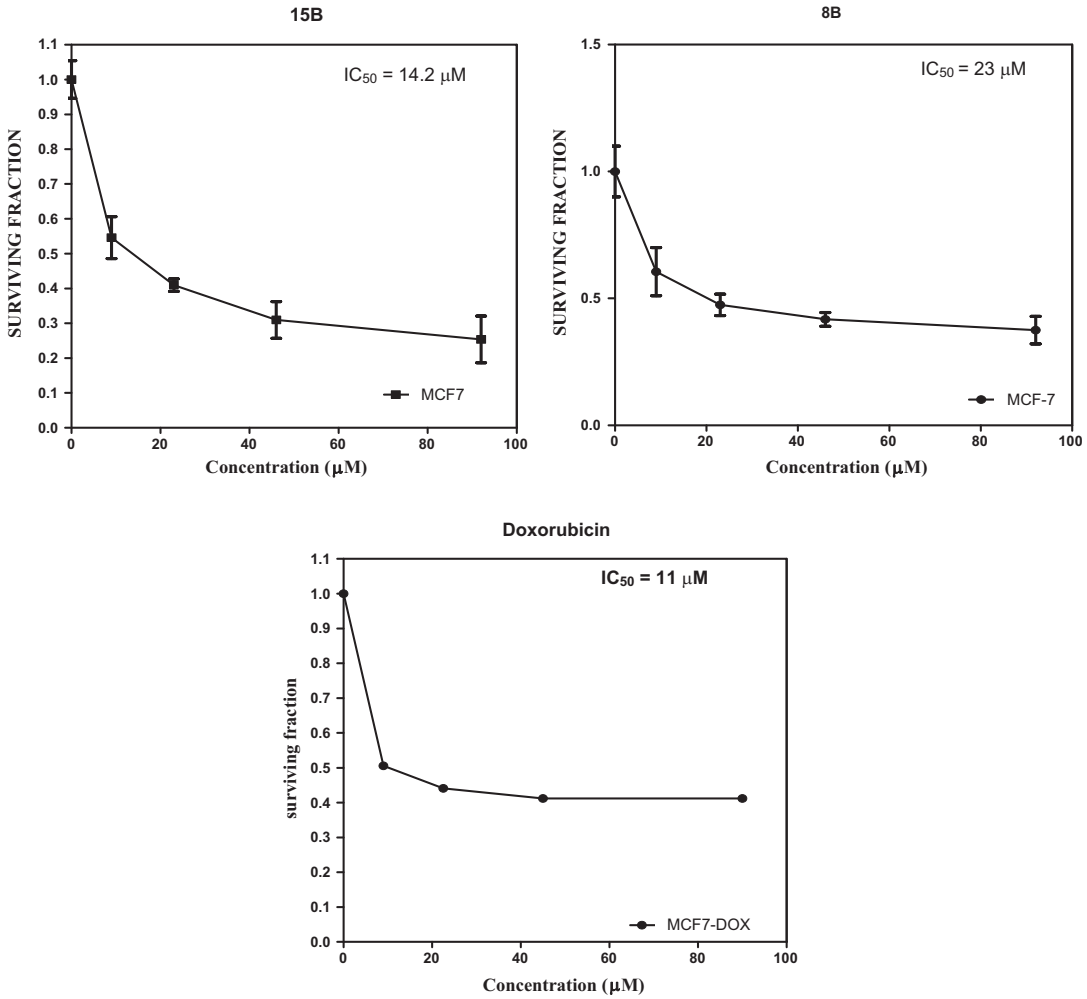

Figure 2. Surviving fractions of MCF-7 cells treated with different concentrations (9–92 μM/mL) of doxorubicin, compounds **15b** and **8b** for 48 h. The results are expressed as the mean ± SD of three independent experiments performed in quadruplicate.

Table 2. Percentage inhibition of 100 μg/mL of the tested compounds on MCF-7 and HEPG-2 cell lines.

Samples (100 μg/mL)	Percentage of inhibition (%)			
	Concn in (μM/mL)	Normal melanocytes (HBF4) (%inhibition)	Liver carcinoma (HEPG-2) (%inhibition)	Human breast cancer (MCF-7) (%inhibition)
8a	243.6	23	39	76
8b	225.1	30	38	79
8c	218.5	24	37	78
11a	229.1	25	37.5	73
11b	206.8	21	37.5	74
14a	229.1	25	30	71
14b	207.2	30	29	76
15a	201.7	35	24	66
15b	184.3	17	25	80

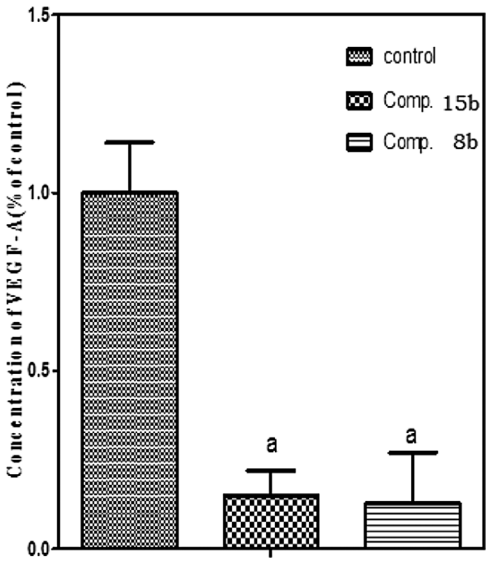

Figure 3. Effects of 14.2 μM/mL of compound **15b**, and 23 μM/mL of compound **8b** on VEGF secretion by MCF-7 cells following 48 h of incubation. Results are expressed as means ± SD of two independent experiments performed in duplicates. Statistical significance of results was analyzed by one way ANOVA using Tukey–Kramer multiple comparison test. [a]Significantly different from the control at P-value < 0.05.

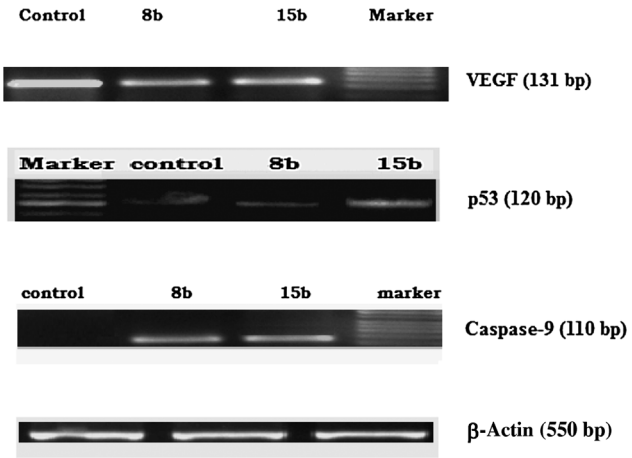

Figure 4. 1.5% agarose gel electrophoresis, showing the effect of compound **15b** ($IC_{50} = 14.2$ μM/mL) and **8b** ($IC_{50} = 23$ μM/mL) on the expression of mRNA of VEGF, β-actin, p53, and caspase-9 in MCF-7 cells 48 h following treatment using RT-PCR analysis.

DNA fragmentation

Genomic DNA was purified from cells treated with 14.2 μM/mL and 23 μM/mL of synthesized compounds **15b** and **8b**, respectively, for 48-h exposure. Then it was subjected to agarose gel electrophoresis to assess DNA fragmentation [30]. DNA fragmentation was observed for the synthesized compounds, where the two tested compounds degrade the DNA samples into two fragments (Fig. 5). We have shown that the synthesized compounds **15b** and **8b** inhibit the growth of human MCF-7 breast adenocarcinoma cells and cause apoptotic DNA fragmentation. This result is similar to that obtained by Arun et al. [15], where the author compounds spirooxindole–pyrrolidines cause DNA fragmentation of A549 cells.

Conclusion

Most of the compounds exhibited high to moderate antimicrobial activity. In addition, they showed more potent cytotoxic effect on human breast cancer MCF-7. Also, we have found that the cyclic 2-oxindole derivatives containing ester group as **8c**, **11b**, **14b**, and **15b** are more promising anticancer drugs than those containing cyanide group as **8a**, **11a**, **14a**, and **15a**). Moreover, the compounds **15b** and **8b** are the most active derivatives in this group. The two compounds **15b** and **8b** induce apoptosis through the induction of caspase-9 and the tumor suppressor protein p53, and also through DNA fragmentation. Finally, these two derivatives decrease VEGF expression and secretion.

Experimental

Chemistry

Melting points were determined on a Stuart melting point apparatus and are uncorrected. The infrared spectroscopy (IR) spectra were recorded as KBr pellets using a Bruker-vector 22 spectrophotometer Fourier transform infrared spectroscopy (FTIR). The ^1H and ^{13}C NMR spectra were recorded in DMSO-d_6 as solvent at 300 MHz and 75 MHz, respectively on Varian Gemini NMR spectrometer using tetramethylsilane (TMS) as internal standard. Chemical shifts are reported in δ units (ppm). Mass spectra were measured on a Shimadzu GMSS -QP-1000 EX mass spectrometer at 70 eV.

*General procedures for compounds **8a–c**, **11a,b**, **14a,b**, and **15a,b***

A mixture of 3-arylamino-5,5-dimethylcyclohex-2-enones **3a–d** (10 mmol) and cyanomethylidine oxindoles **4a,b** was refluxed in dioxane (20 mL) in the presence of piperidine [0.5 mL or DBU (0.5 mL)] for 6 h. The solvent was evaporated under vacuum and the crude product was collected and crystallized from ethanol or ethanol/dioxan.

*2′-Amino-7′,7′-dimethyl-2,5′-dioxo-1′-phenyl-5′,6′,7′,8′-tetrahydro-1′H-spiro[indoline-3,4′-quinoline]-3′-carbonitrile (**8a**)*

Yield: 78%, m.p. > 300°C. IR (KBr, cm^{-1}): 3431, 3323 (NH_2), 2189 (CN), 1718 (CO), 1697 (CO); ^1H NMR (400 MHz, DMSO-d_6): δ, ppm: 0.81, 0.88 (2s, 6H, $2CH_3$), 1.78–2.15 (m, 4H, $2CH_2$), 5.37

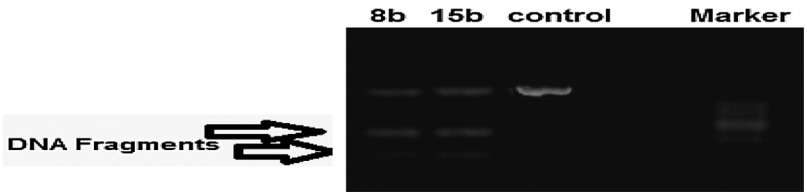

Figure 5. Effect of compounds **8b** and **15b** on MCF-7 cell growth 48 h (cells were treated with 14.2 μM/mL and 23 μM/mL, respectively), and DNA fragmentation was analyzed by 0.8% agarose gel electrophoresis.

(br.s, 2H, NH_2), 6.76–7.76 (m, 9H, Ar-H), 10.22 (s, 1H, NH, D_2O exchangeable); ^{13}C NMR (100 MHz, DMSO-d_6): δ, ppm: 27.1, 28.7, 32.6, 41.8, 48.9, 49.8, 61.3, 109.3, 110.8, 119.4, 121.8, 123.6, 128.1, 130.4, 130.7, 136.4, 137.1, 141.9, 151.6, 152.3, 179.9, 194.4. MS (EI): *m/z* (%) = 410 (M^+). Anal. calcd. for $C_{25}H_{22}N_4O_2$ (410.47): C, 73.15; H, 5.40; N, 13.65. Found: C, 73.36; H, 5.28; N, 13.91.

2′-Amino-1′-(4-chlorophenyl)-7′,7′-dimethyl-2,5′-dioxo-5′,6′,7′,8′-tetrahydro-1′H-spiro[indoline-3,4′-quinoline]-3′-carbonitrile ***(8b)***
Yield: 82%, m.p. > 300°C. IR (KBr, cm^{-1}): 3320, 3315 (NH_2), 2188 (CN), 1744 (CO), 1640 (CO); ^1H NMR (400 MHz, DMSO-d_6): δ, ppm: 0.82, 0.89 (2s, 6H, $2CH_3$), 1.80–2.16 (m, 4H, $2CH_2$), 5.56 (br.s, 2H, NH_2), 6.75–7.67 (m, 8H, Ar-H), 10.21 (s, 1H, NH); ^{13}C NMR (100 MHz, DMSO-d_6): δ, ppm: 27.0, 28.7, 32.6, 41.8, 49.0, 49.8, 61.3, 109.2, 111.0, 119.4, 121.8, 123.7, 128.1, 130.7, 132.4, 134.9, 135.4, 137.1, 141.9, 151.6, 152.1, 179.9, 194.5. MS (EI): *m/z* (%) = 444 (M^+). Anal. calcd. for $C_{25}H_{21}ClN_4O_2$ (444.91): C, 67.49; H, 4.76; Cl, 7.97; N, 12.59. Found: C, 67.57; H, 4.83; Cl, 8.11; N, 12.67.

Ethyl 2′-amino-7′,7′-dimethyl-2,5′-dioxo-1′-phenyl-5′,6′,7′,8′-tetrahydro-1′H-spiro[indoline-3,4′-quinoline]-3′-carboxylate ***(8c)***
Yield: 72%, m.p. 293–295°C. IR (KBr, cm^{-1}): 3367, 3198 (NH_2), 1704 (CO), 1651 (CO); ^1H NMR (400 MHz, DMSO-d_6): δ, ppm: 0.74, 0.85 (2s, 6H, $2CH_3$), 0.83 (t, 3H, CH_3, J = 6.8 Hz), 1.71–1.87 (dd, 2H, CH_2), 1.99–2.17 (m, 2H, CH_2), 3.69 (q, 2H, CH_2, J = 6.8 Hz), 6.63–7.65 (m, 11H, Ar-H and NH_2), 9.92 (s, 1H, NH, D_2O exchangeable); ^{13}C NMR (100 MHz, DMSO-d_6): δ, ppm: 13.6, 26.7, 28.8, 32.1, 42.4, 49.2, 50.6, 59.0, 79.7, 108.1, 113.2, 120.7, 123.1, 127.2, 127.6, 130.4, 130.9, 136.6, 138.3, 144.0, 150.8, 153.1, 169.1, 182.5, 194.1. MS (EI): *m/z* (%) = 457 (M^+). Anal. calcd. for $C_{27}H_{27}N_3O_4$ (457.52): C, 70.88; H, 5.95; N, 9.18. Found: C, 70.67; H, 5.78; N, 9.37.

11′,11′-Dimethyl-2,5′,9′-trioxo-5′,6′,9′,10′,11′,12′-hexahydrospiro[indoline-3,8′-quinolino[1,2-a]-quinazoline]-7′-carbonitrile ***(11a)***
Yield: 75%, m.p. > 300°C. IR (KBr, cm^{-1}): 3308 (NH2), 2194 (CN), 1719 (CO), 1651 (CO), 1598 (CO); ^1H NMR (400 MHz, DMSO-d_6): δ, ppm: 1.02, 1.06 (2s, 6H, $2CH_3$), 2.07–3.34 (m, 4H, $2CH_2$), 6.78–8.0 (m, 8H, Ar-H), 10.58 (s, 1H, NH, D_2O exchangeable), 11.64 (s, 1H, NH, D_2O exchangeable); ^{13}C NMR (100 MHz, DMSO-d_6): δ, ppm: 27.5, 28.0, 32.4, 34.5, 42.4, 50.2, 66.8, 109.9, 111.2, 115.7, 117.8, 120.1, 120.4, 122.3, 123.8, 125.7, 128.0, 129.2, 133.2, 134.7, 137.8, 141.9, 142.5, 151.5, 177.8, 194.5. MS (EI): *m/z* (%) = 436 (M^+). Anal. calcd. for $C_{26}H_{20}N_4O_3$ (436.47): C, 71.55; H, 4.62; N, 12.84. Found: C, 71.36; H, 4.67; N, 12.96.

Ethyl 11′,11′-dimethyl-2,5′,9′-trioxo-5′,6′,9′,10′,11′,12′-hexahydrospiro[indoline-3,8′-quinolino[1,2-a]-quinazoline]-7′-carboxylate ***(11b)***
Yield: 73%, m.p. 296–298°C. IR (KBr, cm^{-1}): 3373 (NH), 1714 (CO), 1687 (CO), 1658 (CO); ^1H NMR (400 MHz, DMSO-d_6): δ, ppm: 0.80 (t, 3H, CH_3, J = 7.08 Hz), 0.94, 1.02 (2s, 6H, $2CH_3$), 1.99–2.31 (m, 4H, $2CH_2$), 3.70 (q, 2H, CH_2, J = 7.08 Hz), 6.63–7.65 (m, 8H, Ar-H), 10.14 (s, 1H, NH, D_2O exchangeable), 11.99 (s, 1H, NH, D_2O exchangeable); ^{13}C NMR (100 MHz, DMSO-d_6): δ, ppm: 13.6, 27.2, 28.2, 32.0, 33.9, 42.8, 59.3, 61.0, 76.8, 87.6, 108.6, 108.9, 113.6, 119.6, 120.9, 122.7, 125.8, 127.6, 134.7, 136.4, 138.0, 144.4, 146.9, 158.7, 159.6, 168.1, 180.4, 195.2. MS (EI): *m/z* (%) = 483 (M^+). Anal. calcd. for $C_{28}H_{25}N_3O_5$ (483.52): C, 69.55; H, 5.21; N, 8.69. Found: C, 69.33; H, 5.47; N, 8.81.

5′-Amino-11′,11′-dimethyl-2,9′-dioxo-9′,10′,11′,12′-tetrahydrospiro[indoline-3,8′-quinolino[1,2-a]-quinazoline]-7′-carbonitrile ***(14a)***
Yield: 84%, m.p. > 300°C. IR (KBr, cm^{-1}): 3307 (NH_2), 2193 (CN), 1709 (CO), 1681 (CO); ^1H NMR (400 MHz, DMSO-d_6): δ, ppm: 0.99, 1.03 (2s, 6H, $2CH_3$), 2.07–2.17 (m, 2H, CH_2), 2.68–2.69 (m, 2H, CH_2), 6.84–7.60 (m, 10H, Ar-H and NH_2), 10.40 (s, 1H, NH); MS (EI): *m/z* (%) = 435 (M^+). Anal. calcd. for $C_{26}H_{21}N_5O_2$ (435.48): C, 71.71; H, 4.86; N, 16.08. Found: C, 71.56; H, 4.62; N, 16.36.

Ethyl 5′-amino-11′,11′-dimethyl-2,9′-dioxo-9′,10′,11′,12′-tetrahydrospiro[indoline-3,8′-quinolino[1,2-a]-quinazoline]-7′-carboxylate ***(14b)***
Yield: 74%, m.p. 290–292°C. IR (KBr, cm^{-1}): 3271, 2960 (NH_2), 1709 (CO), 1686 (CO), 1652 (CO); ^1H NMR (400 MHz, DMSO-d_6): δ, ppm: 0.77, 0.87 (2s, 6H, $2CH_3$), 1.05 (t, 3H, CH_3, J = 7.2 Hz), 1.84–2.20 (m, 4H, 2 CH_2), 3.67 (q, 2H, CH_2, J = 7.2 Hz), 6.63–8.18 (m, 10H, Ar-H and NH_2), 10.43 (s, 1H, NH); MS (EI): *m/z* (%) = 482 (M^+). Anal. calcd. for $C_{28}H_{26}N_4O_4$ (482.54): C, 69.70; H, 5.43; N, 11.61, 15.94. Found: C, 69.85; H, 5.73; N, 11.89.

8-Amino-2,2-dimethyl-2′,4-dioxo-1,2,3,4,9,10,11,12-octahydrospiro[benzo[4′,5′]thieno-[3′,2′:5,6]pyrimido-[1,2-a]quinoline-5,3′-indoline]-6-carbonitrile ***(15a)***
Yield: 81%, m.p. > 300°C. IR (KBr, cm^{-1}): 3307 (NH_2), 2191 (CN), 1736 (CO), 1645 (CO); ^1H NMR (400 MHz, DMSO-d_6): δ,

ppm: 0.89 and 0.96 (2s, 6H, $2CH_3$), 1.84–1.86 (m, 6H, $3CH_2$), 2.0–2.22 (m, 4H, $2CH_2$), 2.78–2.82 (m, 2H, CH_2), 6.08 (br s., 2H, NH_2), 6.77–7.23 (m, 4H, Ar-H), 10.31 (s, 1H, NH) ; ^{13}C NMR (100 MHz, DMSO-d_6): δ, ppm: 21.7, 22.9, 24.3, 24.9, 26.3, 29.1, 32.3, 32.8, 48.7, 49.6, 62.1, 109.5, 114.1, 115.1, 118.7, 122.1, 123.3, 128.5, 135.1, 136.5, 139.9, 142.1, 151.3, 153.9, 159.2, 164.6, 179.7, 194.6 ; MS (EI): *m/z* (%) = 495 (M^+). Anal. calcd. for $C_{28}H_{25}N_5O_2S$ (495.60): C, 67.86; H, 5.08; N, 14.13; S, 6.47. Found: C, 67.93; H, 5.17; N, 14.31; S, 6.52.

*Ethyl 8-amino-2,2-dimethyl-2′,4-dioxo-1,2,3,4,9,10,11,12-octahydrospiro[benzo-[4′,5′]thieno[3′,2′:5,6]pyrimido-[1,2-a]quinoline-5,3′-indoline]-6-carboxylate (**15b**)*
Yield: 76%, m.p. 288–290°C. IR (KBr, cm^{-1}): 3404 (NH_2), 1718 (CO), 1636 (CO), 1625 (CO); ^{1}H NMR (400 MHz, DMSO-d_6): δ, ppm: 0.81 (s, 3H, CH_3), 0,85 (t, 3H, CH_3, $J = 7.08$), 0.92 (s, 3H, CH_3), 1.85–1.97 (m, 8H, $4CH_2$), 2.63–2.89 (m, 4H, $2CH_2$), 3.73 (q, 2H, CH_2, $J = 7.08$), 6.65–7.05 (m, 4H, Ar-H), 7.56 (br s., 2H, NH_2), 10.02 (s, 1H, NH) ; ^{13}C NMR (100 MHz, DMSO-d_6): δ, ppm: 13.6, 21.7, 22.7, 24.3, 25.0, 25.9, 29.1, 32.2, 41.1, 48.9, 50.6, 59.4, 80.6, 108.4, 112.9, 114.0, 114.7, 120.7, 122.7, 127.5, 135.0, 137.6, 140.0, 142.6, 144.1, 150.2, 152.8, 169.1, 181.6, 194.5; MS (EI): *m/z* (%) = 542 (M^+). Anal. calcd. for $C_{30}H_{30}N_4O_4S$ (542.65): C, 66.40; H, 5.57; N, 10.32; S, 5.91. Found: C, 66.28; H, 5.68; N, 10.47; S, 6.11.

Biology

Antimicrobial assay
Antibacterial test of novel derivatives was determined according to Mohamed et al. [31], using a modified Kirby–Bauer disk diffusion method [32]. All synthesized compounds were investigated using two gram-positive bacterial strains as *B. subtilis* and *S. aureus* and two gram-negative strains as *E. coli* and *P. aeruginosa*. Where, 100 μL of all human pathogenic bacteria was grown in 10 mL of fresh media until they reached a count of approximately 10^8 cells/mL [33]. One hundred microliters of bacterial suspension were spread onto agar plates corresponding to the broth in which they were maintained. Blank filter paper disks (Whatman) with a diameter of 11.0 mm were impregnated with 100 μL of tested compound dissolved in 1% DMSO of the stock solutions (30 mg/mL). Disk diffusion method was tested by using approved standard method developed by the National Committee for Clinical Laboratory Standards [34]. Bacterial strains were incubated at 37°C for 24 h. After incubation, the antibacterial activity was measured in terms of the zone of inhibition (IZ) in mm [32]. Standard disks of tetracycline [(standard antibacterial agent served as positive control for antibacterial assay and filter disks impregnated with 100 μL of solvent (DMSO)] were used as a negative control.

SRB analysis
The cytotoxicity was determined according to our previously reported method with few modifications [31], using two different tumor cell lines, human breast cancer (MCF-7) and liver carcinoma HEPG-2; they were obtained from The National Cancer Institute, Egypt. Cells were seeded at a density of 3×10^3 per well in 96-well microtiter plates. Cells were left for 24 h before incubation with 100 μg/mL of the tested compounds for time interval of 48 h. Cytotoxicity was determined using sulforhodamine B (SRB) assay according to previously explained by Skehan et al. [35]. Fixation of cells was performed by the addition of 10% cold trichloroacetic acid. After 1 h incubation at 4°C, cells were washed five times with deionized water. The cells were then stained with 0.4% SRB dissolved in 1% acetic acid for at least 30 min and subsequently washed four times with 1% acetic acid to remove unbound stain. The plates were left to dry at room temperature and bound protein stain was solubilized with 100 μL/well Tris base (10 mM, pH 10.5) and the optical density of each well was measured spectrophotometrically at 570 nm with an ELISA microplate reader (Sunrise Tecan reader, Germany) and the mean value of each drug concentration was calculated. Data from cell viability analysis were analyzed using Prism Software program (GraphPad Software incorporated, version 3) to determine IC_{50} values of the two tested compounds (**15b** and **8b**) against the most sensitive line (MCF-7) after 48 h. In addition, the compounds were tested against the normal cell line HFB4 (normal melanocytes) using the same SRB method.

*Effect of compounds **15b** and **8b** on protein level of VEGF in culture media*
VEGF was determined in cell culture medium using an ELISA kit (RayBiotech, Inc.) according to the method described by Kim et al. [36]. VEGF significantly influences vascular permeability and is a strong angiogenic protein supporting the proliferation of blood vessels. The RayBio Human VEGF ELISA kit is an *in vitro* enzyme-linked immunosorbent assay, which can be used for the quantitation of human VEGF in cell culture supernatant. This assay employs an antibody specific for human VEGF coated on a 96-well plate. VEGF present in samples and standards is bound to the wells by the immobilized antibody. According to the kit manufacturer's instructions, a yellow color is developed, which is proportional to the amount of VEGF bound. The intensity of the color is measured at 450 nm.

Semi-quantitative RT-PCR analysis of VEGF, p53, and caspase-9
RT-PCR analysis was performed according to Liu et al. [37]. Total RNA was extracted from cell cultures (control and treated with synthesized compound **15b** and **8b**), using the Trizol commercial kit (Invitrogen) according to the manufacturer's protocol. Total cDNA was synthesized from the RNA by reverse transcription using specific primers for VEGF, p53, and caspase-9 (primers sequence were shown in Table 3), using high-capacity cDNA archive kit, which was purchased from Applied Biosystems (Foster City, California, USA), following the protocol provided by the manufacturer. Then PT-PCR was done by Qiagen's one step RT-PCR (Hilden, Germany).

Table 3. Primers sequence of VEGF, β-actin, p53, and caspase-9.

Name of gene	Primer sequence
VEGF	Forward: 5′-tcc tcacac cat tgaaac ca-3′ Reverse: 5′-gat cctgccctgtctctc tg-3′
β-Actin	Forward: 5′-gcc gtcttc ccc tccatc gt-3′ Reverse: 5′-tgt cacvgcacgattt ccc tc-3′
p53	Forward: 5′-gttccgagagctgaatgagg-3′ Reverse: 5′-ttatggcgggaggtcgactg-3′
Caspase-9	Forward: 5′-ggctgtctacggcacagatgg-3′ Reverse: 5′-ctggctcggggcggttactgccag-3′

DNA fragmentation

For the DNA fragmentation assay, MCF-7 breast adenocarcinoma cancer cells (3×10^3 cells) (control and treated with synthesized compounds **15b** and **8b**), were collected by centrifugation at 5000 rpm for 7 min and washed twice with phosphate-buffered saline (PBS; Ambion, USA). The extraction procedure was performed according to Biospin Cell Genomic DNA Extraction Kit (Bioflux cat # BSC05S1) with some minor modifications. The cell pellet was suspended in 100 mL of cell lysis buffer. Then the mixture was incubated with proteinase K (Bioflux) at 56°C for 20 min, then incubated with 200 μL of both GA buffer and G-binding buffer + 50 μL ethanol, respectively. The whole mixture was transferred to spin column for centrifugation at 10,000 rpm for 1 min, the remaining steps were performed according to the instructions showed in DNA extraction kit (Bioflux). Finally the eluted DNA was separated by 0.8% agarose gel electrophoresis to assess DNA fragmentation.

Ismail A. Abdelhamid is deeply indebted to the Alexander von Humboldt Foundation, Germany for granting him a postdoctoral fellowship. He is also very thankful to Prof. Dr. Holger Butenschön, Institut für Organische Chemie, Leibniz Universität, Hannover, for kind hospitality.

The authors have declared no conflict of interest.

References

[1] C. V. Galliford, K. A. Scheidt, *Angew. Chem. Int. Ed.* **2007**, *46*, 8748.
[2] T-H. Kang, Y. Murakami, K. Matsumoto, H. Takayama, M. Kitajima, N. Aimi, H. Watanabe, *Eur. J. Pharmacol.* **2002**, *455*, 27e.
[3] C. V. Galliford, K. A. Scheidt, **2007**, *46*, 8748–8758.
[4] H. Lin, S. J. Danishefsky, *Angew. Chem. Int. Ed.* **2003**, *42*, 36–51.
[5] C. Marti, E. M. Carreira, *Eur. J. Org. Chem.* **2003**, 2209–2219.
[6] M. Rottmann, C. McNamara, B. K. S. Yeung, M. C. S. Lee, B. Zou, B. Russell, P. Seitz, D. M. Plouffe, N. V. Dharia, J. Tan, S. B. Cohen, K. R. Spencer, G. E. Gonza, lez-Paez, S. B. Lakshminarayana, A. Goh, R. Suwanarusk, T. Jegla, E. K. Schmitt, H.-P. Beck, R. Brun, F. Nosten, L. Renia, V. Dartois, T. H. Keller, D. A. Fidock, E. A. Winzeler, T. T. Diagana, *Science* **2010**, *329*, 1175–1180.
[7] B. K. S. Yeung, B. Zou, M. Rottmann, S. B. Lakshminarayana, S. H. Ang, S. Y. Leong, J. Tan, J. Wong, S. Keller-Maerki, C. Fischli, A. Goh, E. K. Schmitt, P. Krastel, E. Francotte, K. Kuhen, D. Plouffe, K. Henson, T. Wagner, E. A. Winzeler, F. Petersen, R. Brun, V. Dartois, T. T. Diagana, T. H. Keller, *J. Med. Chem.* **2010**, *53*, 5155–5164.
[8] A. R. Gholap, K. S. Toti, F. Shirazi, R. Kumari, M. K. Bhat, M. V. Deshpande, K. V. Srinivasan, *Bioorg. Med. Chem.* **2007**, *15*, 6705–6715.
[9] H. M. Faidallah, A. A. Saqer, K. A. Alamry, K. A. Khan, A. M. Asiri, *J. Enzym Inhib Med. Chem.* **2014**, *29*, 367–378.
[10] S. L. Alqasoumi, A. M. Al-Taweel, A. M. Alafeefy, M. M. Hamed, E. Noaman, M. M. Ghorab, *Bioorg. Med. Chem. Lett.* **2009**, *19*, 6939–6942.
[11] N. S. El-Gohary, *Med. Chem. Res.* **2013**, *22*, 5236–5247.
[12] M. S. Al-Said, M. M. Ghorab, M. S. Al-Dosari, M. M. Hamed, *Eur. J. Med. Chem.* **2011**, *46*, 201–207.
[13] M. M. Ghorab, F. A. Ragab, H. I. Heiba, R. K. Arafa, E. M. El-Hossary, *Med. Chem. Res.* **2011**, 388–400.
[14] A. Jemal, R. Siegel, E. Ward, T. Murray, J. Xu, M. J. Thun, *CA Cancer J. Clin.* **2007**, *57*, 43–66.
[15] Y. Arun, K. Saranraj, C. Balachandran, P. T. Perumal, *Eur. J. Med. Chem.* **2014**, *74*, 50–64.
[16] A. J. Levine, *Cell* **1997**, *88*, 323–331.
[17] W. S. El-Deiry, *Cancer Biol.* **1998**, *8*, 345–357.
[18] B. Vogelstein, D. Lane, A. J. Levine, *Nature* **2000**, *408*, 307–310.
[19] K. Kuida, *Int. J. Biochem. Cell Biology* **2000**, *32*, 121–124.
[20] S.A.S. Ghozlan, I.A. Abdelhamid, M.H. Elnagdi, *Arkivoc xiii* **2006**; 147–157.
[21] a) S. A. S. Ghozlan, I. A. Abdelhamid, H. M. Hassaneen, M. H. Elnagdi, *J. Hetyocycl. Chem.* **2007**, *44*, 105–108. b) I.A. Abdelhamid, *Synlett* **2009**; 625–627.
[22] S. A. S. Ghozlan, M. H. Mohamed, A. M. Abdelmoniem, I. A. Abdelhamid, *Arkivoc* **2009**, *x* 302–311.
[23] I. A. Abdelhamid, M. H. Mohamed, A. M. Abdelmoniem, S. A. S. Ghozlan, *Tetrahedron* **2009**, 10069.
[24] I. A. Abdelhamid, E. S. Darwish, M. A. Nasra, F. M. Abdel-Gallil, D. H. Fleita, *Synthesis* **2010**, 1107.
[25] a) Z. Karimi-Jaberi, Z. Takmilifard, *Eur. Chem. Bull.* **2013**, *2*, 211–213. b) B. Cui, R-H. Wang, L-Z. Chen, Y. Jin, B. Cui, R-H. Wang, L-Z. Chen, Y. Jin, G-F. Han, *Synth. Commun.* **2011**, *41*, 1064–1070. c) B. V. Lichitsky, S. N. Ivanov, A. A. Dudinov, S. A. Woznesensky, M. M. Krayushkin, *Russ. Chem. Bull.* **2001**, *50*, 2428–2432.
[26] A. L. Koch, *Clin. Microbiol. Rev.* **2003**, *16*, 673.
[27] H. J. Smith, C. Simons, *Proteinase and Peptidase Inhibition:Recent Potential Targets for Drug Development*, Taylor and Francis, **2002**, 1–440.

[28] P. Carmeliet, R. Jain, *Nat. Med.* **2000**, *407*, 249–257.
[29] J. M. Vicencio, L. Galluzzi, N. Tajeddine, C. Ortiz, A. Criollo, E. Tasdemir, E. Morselli, A. H. Wyllie, *Mol. Neurobiol.* **2010**, *42*, 4–9.
[30] H. Akiyama, M. Endo, T. Matsui, I. Katsuda, N. Emi, Y. Kawamoto, T. Koike, H. Beppu, *Biochim. Biophys. Acta Gen. Subj.* **2011**, *1810*, 519e.
[31] M. F. Mohamed, M. S. Mohamed, S. A. Shouman, M. M. Fathi, I. A. Abdelhamid, *Appl. Biochem. Biotechnol.* **2012**, *168*, 1153–1162.
[32] A. W. Bauer, W. M. Kirby, C. Sherris, M. Turck, *Am. J. Clin. Pathol.* **1966**, *45*, 493–496.
[33] M. A. Pfaller, L. Burmeister, M. A. Bartlett, M. G. Rinaldi, *J. Clin. Microbiol.* **1988**, *26*, 1437–1441.
[34] National for Laboratory Standards, 2003, Method for antifungal disk diffusion susceptibility testing of yeast: proposed guideline M44-P. Wayne.
[35] P. Skehan, R. Storeng, D. Scudiero, A. Monks, J. McMahon, D. Vistica, J. Warren, H. Bokesch, S. Kenney, M. R. Boyd, *J. Nat. Cancer Inst.* **1990**, *82*, 1107–1112.
[36] K. J. Kim, B. Li, K. Houck, J. Winer, N. Ferrara, *Growth Factors* **1992**, *7*, 53–64.
[37] Q. Liu, J. J. Wang, Y. C. Pan, L. F. Meng, X. Zhan, X. Zheng, Q. F. Zheng, *Ai Zheng* **2008**, *27*, 25–29.